ChemComm

COMMUNICATION

View Article Online
View Journal

Cite this: DOI: 10.1039/c4cc08593k

Received 30th October 2014,
Accepted 2nd December 2014

DOI: 10.1039/c4cc08593k

www.rsc.org/chemcomm

Amide–triazole isosteric substitution for tuning self-assembly and incorporating new functions into soft supramolecular materials†

Jürgen Bachl,‡[a] Judith Mayr,‡[a] Francisco J. Sayago,[b] Carlos Cativiela[b] and David Díaz Díaz*[ac]

The proof-of-concept for the modular synthesis of new functional soft gel materials based on amide–triazole isosteric replacement has been demonstrated. A coassembly approach of isosteric amino acid-based hydrogelators was fruitfully applied for fine-tuning the release of entrapped drugs.

Bioisosteric replacement is one of the most important tools in medicinal chemistry for the rational design of new drugs.[1,2] The origins of isosterism can be traced back to the early twentieth century to the pioneering work of Langmuir in which he coined this concept to define atoms or molecules which possess the same number and/or arrangement of electrons.[3] Thereafter, Grimm's hydride displacement law[4] and Erlenmeyer's work[5] paved the way to the definition of bioisosteres, largely spread by Friedman[6] and Thornber[7] and later broadened by Burger[8] as "compounds or groups that possess near-equal molecular shapes and volumes, approximately the same distribution of electrons, and which exhibit similar physical properties...".

Nowadays, bioisosteric replacement of amide bonds represents a key strategy in modern research due to its implications in peptide chemistry.[9] Within this context, many promising approaches introducing acyclic esters, thioamides, ureas, carbamates, sulphonamides, oxadiazoles and triazoles have been successfully applied to improve the activity of known drugs or to create new bioactive compounds and materials.[2,10] Among these examples, disubstituted 1,2,3-triazoles have been considered as powerful non-classical isosteres of amides as they can mimic either a *trans*- or a *cis*- configuration of the amide bond depending on the substitution pattern of the triazole (1,4- or 1,5-, respectively).[11,12] Their planar structure exhibits the ability of H-bonding due to the presence of both donor and acceptor groups with similar relative positions. Although the distance R^1–R^2 in *trans*-amides is *ca.* 1 Å shorter than that in 1,4-disubstituted triazoles, the overall dipolar moment of the latter (*ca.* 5.0 D) is slightly larger than that of secondary amides (*ca.* 3.5–4.0 D). Moreover, the H-bonding abilities (oxygen lone pair electrons = acceptor; N–H amide bond = donor) can be mimicked by the N-2/N-3 lone pairs (acceptor) and the triazole C–H bond (donor) (Fig. 1). Calculations in the gas phase have also suggested that the lone pair on N-3 may be a better H-bond acceptor and metal coordination center than N-2. In addition, the potential β-turn geometry of 1,4-disubstituted triazoles has been supported by computational studies.[13] A similar analysis can be done between *cis*-amides and 1,5-disubstituted 1,2,3-triazoles (Fig. S1, ESI†). Besides the application of triazoles in peptidomimetics and bioconjugation, they have also been proven to be useful structural moieties for the fabrication of functional materials.[14,15]

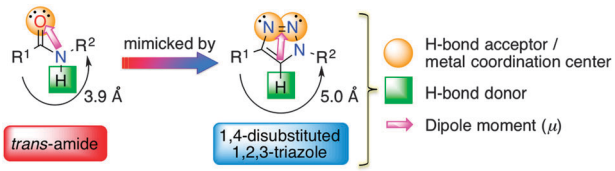

Fig. 1 Main structural features of disubstituted *trans*-amides and 1,2,3-triazoles for their consideration as bioisosteres.

As part of our research program conceived to expand the conceptual toolbox for the development of advanced functional materials, we report here the proof-of-concept demonstration for the synthesis of novel supramolecular soft gel materials based on amide–triazole isosteric substitution.

Fig. 2 shows the structure of the compounds synthesized for this study. *N*-Stearoyl-L-glutamic acid (**C_{18}-Glu**) is an amphiphilic compound that has been reported to self-assemble into nanofibers in chloroform and nanodisc-like structures in 1 : 1 mixed EtOH–H_2O.[16] We envisioned that this molecule could also undergo self-assembly in many other solvents at suitable concentrations. In addition, it provided us with a unique opportunity to assess the transplantation

[a] *Universität Regensburg, Fakultät für Chemie und Pharmazie, Institut für Organische Chemie, Universitätsstr. 31, 93053 Regensburg, Germany. E-mail: David.Diaz@chemie.uni-regensburg.de*
[b] *Instituto de Síntesis Química y Catálisis Homogénea (ISQCH), CSIC-Universidad de Zaragoza, 50009 Zaragoza, Spain*
[c] *IQAC-CSIC, Jordi Girona 18-26, Barcelona 08034, Spain*

† Electronic supplementary information (ESI) available: Full experimental details, tabular data, expanded discussion, additional plots, figures and expanded literature. See DOI: 10.1039/c4cc08593k

‡ These two authors are equal main contributors.

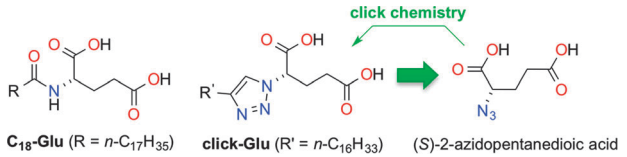

Fig. 2 Model compounds **C_{18}-Glu** and **click-Glu** derived from L-glutamic acid used in this work.

of the isosteric replacement paradigm from medicinal chemistry to soft materials. Thus, the analogue **click-Glu**, in which the 1,4-disubstituted 1,2,3-triazole unit has formally replaced the amide moiety in **C_{18}-Glu** keeping the total number of C atoms intact, was easily synthesized *via* click chemistry[17] by the copper(I)-catalyzed azide–alkyne cycloaddition. The synthesis of this compound required prior preparation of (*S*)-2-azidopentanedioic acid from the corresponding L-glutamic acid using imidazole-1-sulfonyl azide hydrochloride as the diazo transfer reagent (Section S3.2, ESI†).

The gelation ability of **C_{18}-Glu** and **click-Glu** was systematically investigated by applying a heating–cooling cycle in H_2O and 25 organic solvents (including non-polar, polar protic and polar aprotic solvents). Materials that did not exhibit gravitational flow upon turning the vial upside-down were preliminary classified as stable gels. No visible changes were observed in model examples upon one-year of aging, and their gel nature was further confirmed by dynamic rheological measurements (*vide infra*). In general, more than 10 different gels could be obtained with both gelators in oxygenated, hydrocarbon (including aromatic and aliphatic) and halogenated solvents. However, some exceptions were also found in most types of solvents leading to the formation of precipitates, clear solutions or partial gels after cooling down the corresponding isotropic solutions (*e.g.*, 1-hexanol, DMF, THF, EtOAc, 1,4-dioxane, acetone, chlorobenzene, benzonitrile, and silicon oil). Interestingly, only **click-Glu** was able to form stable gels in DMSO, EtOH and i-PrOH, expanding the gelation scope in comparison to **C_{18}-Glu** (Table S1, ESI†). The remarkable gelation tendency of **click-Glu** was also revealed by fast *in situ* gelation of DMSO–H_2O mixtures during its synthesis (Fig. S5, ESI†). In agreement with the possible formation of particle aggregates larger than the wavelength of visible light (*ca.* 350–750 nm), most gels exhibited an opaque white appearance except for those obtained in glycerol, which were translucent (Fig. 3).

Despite the fact that many solvents could be gelled by either **C_{18}-Glu** or **click-Glu**, the critical gelation concentration (CGC),

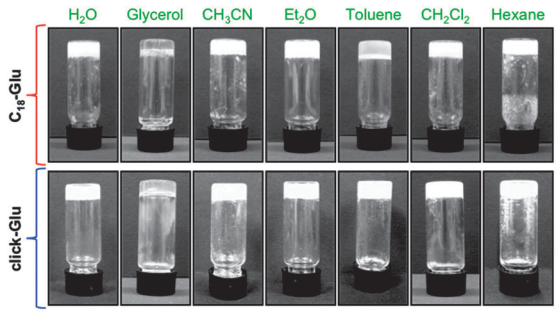

Fig. 3 Selected digital photographs of upside-down vials containing stable gels prepared from **C_{18}-Glu** and **click-Glu** at their corresponding critical gelation concentrations (see the ESI† for additional pictures and details).

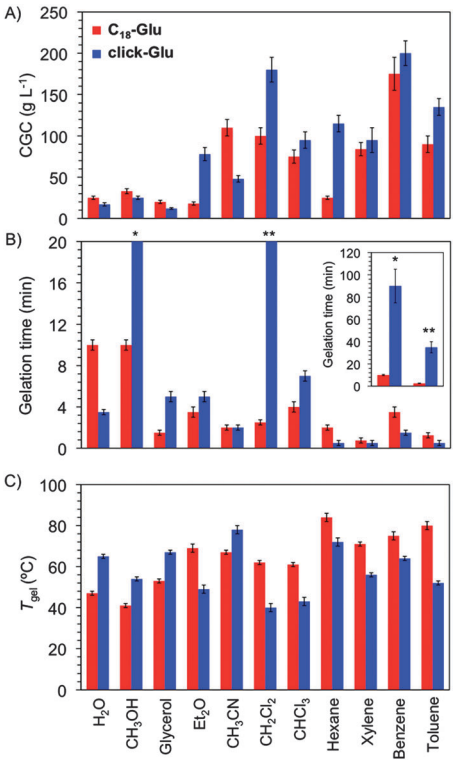

Fig. 4 Comparative graphs of the (A) CGC, (B) gelation time and (C) T_{gel} of gels prepared from **C_{18}-Glu** and **click-Glu**. Time and T_{gel} values were measured at the same gelator concentration defined by the higher CGC in each case (see the ESI† for details and additional data).

thermal stability and gelation kinetics were different in each case (Fig. 4; Table S1, ESI†). CGC values were established in the range of 10–200 g L^{-1} in most cases. Nevertheless, **click-Glu** generally exhibited *ca.* 25–55% lower CGC values than **C_{18}-Glu** when polar protic and polar aprotic solvents were used (*e.g.*, H_2O, CH_3OH, glycerol, and CH_3CN). On the other hand, an opposite behavior (*ca.* 10–75% higher CGC) was usually observed in non-polar solvents (*e.g.*, Et_2O, CH_2Cl_2, *n*-hexane, and toluene) (Fig. 4A). The above results already constituted a clear indication of the significant impact that the amide–triazole isosteric replacement could have on the self-assembly properties of the gelators.

Although most gels were obtained within minutes regardless of the gelator structure, the gelation kinetics was found to be significantly slower in polar solvents. Taking H_2O and $CHCl_3$ as polar and non-polar model solvents for further discussion, Ln–Ln plots of gelation-time *vs.* gelator-concentration revealed that for an equivalent increment in the concentration with respect to the CGC, the gelation rate was nearly identical either in water or $CHCl_3$ for both gelators. However, **click-Glu** showed faster absolute gelation kinetics in water than **C_{18}-Glu** at the corresponding CGC (Table S1, ESI†). Similarly, shorter gelation times were generally observed for **C_{18}-Glu** in non-polar solvents (Fig. 4B).

Independent of the nature of the solvent or the gelator, all gels exhibited full thermo-reversibility with gel-to-sol transition temperatures (T_{gel}) in the range of *ca.* 40–70 °C as indicated by DSC among other techniques (Fig. S7, ESI†). Remarkably, some T_{gel} values exceeded the boiling points of the corresponding solvents

(*e.g.*, *n*-hexane, bp = 69 °C; T_{gel} (**C_{18}-Glu**) = 84 ± 2 °C; T_{gel} (**click-Glu**) = 72 ± 2 °C). Similar to the trends observed for CGC-values, materials derived from **click-Glu** generally exhibited, at comparable concentrations, higher T_{gel} values in polar solvents than those obtained from **C_{18}-Glu**, which were superior in non-polar solvents (Fig. 4C). Up to 40% increase of T_{gel} could be observed when the gelator and solvent polarities matched.

As expected, T_{gel} increased with the increasing gelator concentration regardless of the solvent or the gelator, which is in agreement with the gradual formation of denser packed supramolecular networks. The concentration of **C_{18}-Glu** could be increased up to 500 g L^{-1} in both model solvents affording homogeneous gels, whereas the concentration of isosteric **click-Glu** could be increased even up to 700 g L^{-1} in $CHCl_3$ and 900 g L^{-1} in water. Obvious plateau regions for all examples (ΔT_{gel} = 20–33 °C) were reached before the gels collapsed. Ln–Ln plots before the plateau regions showed a clear linear relationship between the increment in the gelator concentration and the consequent increment in the T_{gel} with respect to the initial values at the CGC. Within the end limits defined by the CGCs and the maximum T_{gel} values, the slopes of these straight lines indicated that a 1.3-fold higher percentage increment of T_{gel} could be obtained either in water or $CHCl_3$ when **C_{18}-Glu** or **click-Glu** are used as gelators, respectively (Fig. S9, ESI†).

In terms of gel stability towards chemical additives, the hydrogels made from **click-Glu** at the CGC remained stable under neutral and acidic conditions, whereas irreversible gel-to-sol phase transitions could be observed by mechanical agitation or addition of NaOH, electrolytes, buffers or certain organic solvents. Organogels made from **click-Glu** and organo-/hydrogels made from **C_{18}-Glu** behaved similarly, albeit they showed a considerable stability in the presence of electrolytes and phosphate buffered saline (PBS) solutions (Fig. S10, ESI†).

Oscillatory rheological measurements (*i.e.*, DFS, DSS and DTS experiments) of representative gels unequivocally confirmed their viscoelastic nature. Within the linearity limits of deformation, the storage modulus G' was approximately one order of magnitude higher than the loss modulus G'' (Table 1). Destruction of the gels at low frequency and below 10% strain indicated the brittle nature of the materials. DTS measurements at 0.1% strain and 1 Hz frequency confirmed the stability of the gel materials as a function of the ageing time at room temperature. In general, the tan δ (G''/G') values among random measurements of the same material were reproducible and decreased with the concentration of the gelator, suggesting an enhancement of the mechanical damping properties. Well aligned to the impact of the gelator structure on both the CGC and T_{gel} (*vide supra*), **C_{18}-Glu** provided gel materials with higher mechanical strength in aprotic solvents like $CHCl_3$, as indicated by higher absolute G'-values, lower tan δ and higher maximum strain values at break. However, an exact opposite behavior could be observed in polar protic solvents like water, where **click-Glu** exhibited superior properties (Table 1; Fig. S13, ESI†).

Table 1 Summary of rheological properties of model gels[a]

Gelator	Solvent	G' (kPa)	G'' (kPa)	tan δ	γ (%)
C_{18}-Glu	H_2O	15 ± 1.8	4 ± 0.2	0.30 ± 0.01	6 ± 1.3
C_{18}-Glu	$CHCl_3$	778 ± 6.0	101 ± 1.9	0.13 ± 0.01	4 ± 0.8
click-Glu	H_2O	102 ± 10.6	19 ± 0.4	0.19 ± 0.02	9 ± 1.4
click-Glu	$CHCl_3$	109 ± 1.7	45 ± 4.0	0.41 ± 0.03	2 ± 0.7

[a] Gelator concentrations: 25 g L^{-1} (H_2O), 100 g L^{-1} ($CHCl_3$). See ESI.

Electron microscopy imaging was used in order to gain visual insight into the morphologies of model gels (Fig. 5; Fig. S11, ESI†). In good agreement with previous observations,[16] FESEM images of the xerogels based on **C_{18}-Glu** in a polar-protic environment revealed the formation of nanoalmond-like structures with diameters in the range of 1–5 μm, whereas layered lamellar assemblies *ca.* 5–10 μm in width and 15–50 μm in length were observed in $CHCl_3$. Fused nanofibrillar structures with diameters in the range of 30–50 nm were identified as the smallest features in these aggregates. A practically opposite behavior was observed for materials based on the isosteric **click-Glu**. Thus, wrinkled lamellar structures few μm in length and 100–500 nm in width were observed in water, whereas almond crunch-like structures with diameters between hundreds of nm up to few μm were revealed in $CHCl_3$. In general, dense fibrillar networks of high aspect ratios were also observed by TEM imaging. When **click-Glu** was used as the gelator, the density of the fibrillar bundles was much higher than observed in the case of **C_{18}-Glu**. In good agreement, gas-adsorption measurements revealed that materials derived from **C_{18}-Glu** possess a 2.4-fold higher porosity than those obtained from the analogue **click-Glu** (53.4 m^2 g^{-1} and 22.6 m^2 g^{-1}, respectively) (Fig. S12, ESI†).

In agreement with previous observations,[16] the formation of distinctive nanostructures could be explained by different H-bonding patterns caused by either polar protic or non-polar environments. Thus, protic environments apparently favor the assembly of **C_{18}-Glu** in molecular multilayers resembling nanoalmond crunch-like structures mainly due to intermolecular H-bonding between the amide NH-bond and the CO-group of the acid moiety next to the chiral centre, whereas non-polar solvents lead to the formation of nanofibers in which both intermolecular H-bonding and intramolecular H-bonding are nearly equally important.[16] The opposite tendency was observed for **click-Glu**, suggesting that the isosteric replacement can be used to trigger the formation of desired nanostructures in specific solvents (Fig. S14, ESI†). The evidence of such divergent assembly mechanisms of the two isosteres associated to different H-bonding arrangements depending on the solvent nature was also obtained from FT-IR measurements using H_2O and $CHCl_3$ as model solvents (Section S7, ESI†).

At this point, hydrogels prepared from **C_{18}-Glu** and **click-Glu** were preliminary evaluated as carriers for tuning the kinetics of drug release. Vancomycin, a useful glycopeptidic antibiotic for

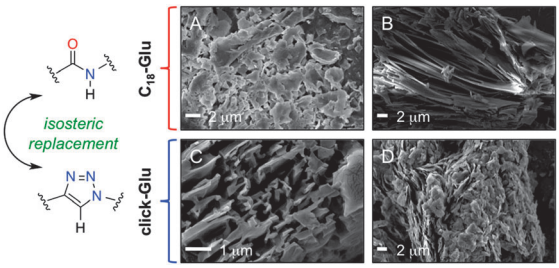

Fig. 5 FESEM images of xerogels prepared by freeze drying the corresponding gels. (A) **C_{18}-Glu** in H_2O (25 g L^{-1}); (B) **C_{18}-Glu** in $CHCl_3$ (100 g L^{-1}); (C) **click-Glu** in H_2O (25 g L^{-1}); (D) **click-Glu** in $CHCl_3$ (100 g L^{-1}).

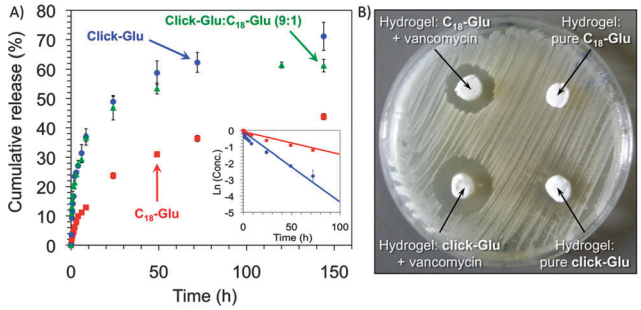

Fig. 6 (A) Release profile of vancomycin in a PBS buffer from hydrogels based on **click-Glu**, $\mathbf{C_{18}}$**-Glu** and coassembled **click-Glu** : $\mathbf{C_{18}}$**-Glu** (9 : 1, w/w). (B) The zone of inhibition test against *Staphylococcus aureus* for vancomycin-containing hydrogel samples and their corresponding controls.

the treatment of infections mostly caused by Gram-positive bacteria, was selected as hydrophilic model drug for this study.[18] Stable hydrogels towards a PBS buffer could be obtained using a gelator concentration of 60 g L^{-1} (Sections S2.2 and S14, ESI†). Thus, we used these conditions for preliminary studies of the release kinetics of entrapped vancomycin (initial drug concentration in the gel phase = 1.38×10^{-3} M). Up to 90% drug release was observed within 13 days in the case of **click-Glu**, whereas $\mathbf{C_{18}}$**-Glu** showed much slower kinetics (*ca.* 56% within the same period). In general, release kinetics obeyed a first-order integrated rate law reasonably well (k_{obs} [$\mathbf{C_{18}}$**-Glu**] = $1.5 \pm 0.2 \times 10^{-2}$ h^{-1}; k_{obs} [**click-Glu**] = $4.3 \pm 0.3 \times 10^{-2}$ h^{-1}) (Fig. 6). These results can be associated with different diffusion properties of the drug through hydrogels with diverse nano-morphologies, which are ultimately governed by the isosteric gelator structure (obviously, the interaction patterns between solvent–gelator, gelator–gelator and gelator/fibril-drug molecules play a key role in such a complex scenario). As expected, a faster release rate was also observed upon decreasing the gelator concentration due to the decrease of the crosslink density of the network (Fig. S16A, ESI†). Remarkably, the complementary structure of the isosteric gelators allowed the preparation of stable hydrogels *via* coassembly of both gelators at different ratios, offering an alternative tuning option for fine-tuning the drug release (Fig. 6A). However, the change in the kinetics upon coassembly was not proportional to the molar ratio of the gelator (Fig. S16B, ESI†), suggesting the formation of complex interpenetrated networks and release kinetics that will be a subject of future studies. The antimicrobial activities of the hydrogels with and without vancomycin against the Gram-positive bacteria *Staphylococcus aureus* were evaluated using the Kirby–Bauer test (Fig. 6B). Large inhibition zones (21.5 mm and 18 mm for drug-loaded **click-Glu** and $\mathbf{C_{18}}$**-Glu**, respectively) were observed. The results were in good agreement with the faster release kinetics of **click-Glu** hydrogels *vs.* $\mathbf{C_{18}}$**-Glu**. No inhibition zones were evident with control gel samples. Maintenance of antimicrobial activity of the released drug was also confirmed (Fig. S18, ESI†).

Finally, it is worth mentioning that the amphiphilic character of the gelators also allowed the entrapment of other drugs with a completely different hydrophilic/hydrophobic balance (*i.e.*, anti-cancer drugs methotrexate, camptothecin and flutamide) and their further release at different rates depending on the isostere used to prepare the gels (Fig. S17, ESI†).

In conclusion, the isosteric replacement paradigm from medicinal chemistry can be successfully applied to the synthesis of novel soft functional materials. As a proof-of-concept, isosteric gelators $\mathbf{C_{18}}$**-Glu** and **click-Glu** afforded the preparation of a variety of physical hydrogels and organogels with different thermal, mechanical, morphological and diffusional properties. In general, **click-Glu** revealed superior features with respect to the CGC, T_{gel} and mechanical stabilities in polar protic solvents, whereas $\mathbf{C_{18}}$**-Glu** exhibited improved properties in non-polar solvents. Moreover, the coassembly of both isosteres was successfully applied for fine-tuning the release of the antibiotic vancomycin. Studies involving the 1,5-disubstituted triazole-based gelators[19] as well as computational calculations to gain deeper insights into the gelation mechanisms and gel properties are currently underway in our lab. Overall, these results open up many exciting opportunities for the development of new functional materials with unique properties for different applications beyond the field of gels.

Financial support from DFG (DI 1748/3-1), Universität Regensburg, Ministerio de Economía y Competitividad-FEDER (grants CTQ2010-17436, CTQ2013-40855-R) and Gobierno de Aragón-FSE (research group E40) is gratefully acknowledged. We thank Dr R. Banerjee and S. Saha (NCL, Pune) for gas-adsorption measurements and Prof. Minghua Liu (ICCAS, Beijing) for his valuable advice on the isolation of $\mathbf{C_{18}}$**-Glu**. We are indebted to Prof. J. Schlossmann, Prof. F. Kees and Astrid Seefeld (Department of Pharmacology and Toxicology, Universität Regensburg) for their generous assistance with the antimicrobial studies. D.D.D. thanks DFG for the Heisenberg Professorship Award.

Notes and references

1 S. R. Langdon, P. Ertl and N. Brown, *Mol. Inf.*, 2010, **29**, 366, and references therein.
2 *Bioisosteres in Medicinal Chemistry*, ed. N. Brown, Wiley-VCH, Weinheim, 2012, vol. 54.
3 I. Langmuir, *J. Am. Chem. Soc.*, 1919, **41**, 1543.
4 H. G. Grimm, *Naturwissenschaften*, 1929, **17**, 557.
5 H. Erlenmeyer and M. Leo, *Helv. Chim. Acta*, 1932, **15**, 1171.
6 H. L. Friedman, *NASNRS*, 1951, **206**, 295.
7 C. W. Thornber, *Chem. Soc. Rev.*, 1979, **8**, 563.
8 A. Burger, *Prog. Drug Res.*, 1991, **37**, 287.
9 (*a*) Y. L. Angell and K. Burgess, *Chem. Soc. Rev.*, 2007, **36**, 1674; (*b*) J. M. Holub and K. Kirshenbaum, *Chem. Soc. Rev.*, 2010, **39**, 1325; (*c*) M. Corredor, J. Bujons, M. Orzáes, M. Sancho, E. Peréz-Payá, I. Alfonso and A. Messeguer, *Eur. J. Med. Chem.*, 2013, **63**, 892.
10 Y. Hamada and Y. Kiso, *Expert Opin. Drug Discovery*, 2012, **7**, 903.
11 G. C. Tron, T. Pirali, R. A. Billington, P. L. Canonico, G. Sorba and A. A. Genazzani, *Med. Res. Rev.*, 2008, **28**, 278.
12 H.-F. Chow, K.-N. Lau, Z. Ke, Y. Liang and C.-M. Lo, *Chem. Commun.*, 2010, **46**, 3437, and references therein.
13 K. Oh and Z. A. Guan, *Chem. Commun.*, 2006, 3069.
14 M. Juricek, P. H. J. Kouwer and A. E. Rowan, *Chem. Commun.*, 2011, **47**, 8740, and references therein.
15 D. D. Díaz, J. J. Cid, P. Vázquez and T. Torres, *Chem. – Eur. J.*, 2008, **14**, 9261and references therein.
16 P. Gao, C. Zhan, L. Liu, Y. Zhou and M. Liu, *Chem. Commun.*, 2004, 1174.
17 V. V. Rostovtsev, L. G. Green, V. V. Fokin and K. B. Sharpless, *Angew. Chem., Int. Ed.*, 2002, **41**, 2596.
18 D. J. Overstreet, R. Huynh, K. Jarbo, R. Y. McLemore and B. L. Vernon, *J. Biomed. Mater. Res.*, 2013, **101**, 1437, and references therein.
19 Several examples of triazole-based gels are given in the ESI.† For representative examples, see: (*a*) H.-F. Chow, C.-M. Lo and Y. Chen, *Top. Heterocycl. Chem.*, 2012, **28**, 137, and references therein; (*b*) A. Hemamalini and T. M. Das, *New J. Chem.*, 2013, **37**, 2419.

